Dissolved Organic Carbon (DOC) in Ground Ice on Northeastern Tibetan Plateau

Yuzhong Yang[1,2], Xiaoyan Guo[3,4,5]*, Qingfeng Wang[1], Huijun Jin[1], Hanbo Yun[1] and Qingbai Wu[2]*

[1]State Key Laboratory of Frozen Soil Engineering, Northwest Institute of Eco-Environment and Resources, Chinese Academy of Sciences, Lanzhou, China, [2]Beiluhe Observation Station of Frozen Soil Environment and Engineering, Northwest Institute of Eco-Environment and Resource, Chinese Academy of Science, Lanzhou, China, [3]Key Laboratory of Ecohydrology of Inland River Basin, Northwest Institute of Eco–Environment and Resources, Chinese Academy of Sciences, Lanzhou, China, [4]Alax Desert Eco-hydrology Experimental Research Station, Lanzhou, China, [5]Qilian Mountains Eco–Environment Research Center in Gansu Province, Beijing, China

Ground ice in permafrost stores substantial amounts of dissolved organic carbon (DOC) upon thaw, which may perpetuate a carbon feedback in permafrost regions, yet little is known to date about the dynamics of DOC and source variability of ground ice on the Tibetan Plateau. Here, the high-resolution data of DOC in ground ice (4.8 m in depth) from two permafrost profiles on the Northeastern Tibetan Plateau (NETP) were firstly presented. We quantified the DOC concentrations (mean: 9.7–21.5 mg/L) of ground ice and revealed sizeable—by a factor of 7.0–36.0—enrichment of the ground ice relative to the other water elements on the TP. Results indicated remarkable depth differences in the DOC of ground ice, suggestive of diverse sources of DOC and different sequestration processes of DOC into ice during permafrost evolution. Combined with DOC and carbon isotopes ($\delta13CDOC$), we clarified that decomposition of soil organic matter and leaching of DOC from organic layers and surrounding permafrost sediments are the important carbon sources of ground ice. The DOC sequestration of ground ice in the upper layers was related to the active layer hydrology and freeze–thaw cycle. However, the permafrost evolution controlled the decomposition of organic carbon and sequestration of DOC in the deep layers. A conceptual model clearly illustrated the dynamics of DOC in ground ice and suggested a significant impact on the carbon cycle on the NETP. The first attempt to explore the DOC in ground ice on the NETP is important and effective for further understanding of carbon cycle under permafrost degradation on the Tibetan Plateau.

Keywords: ground ice, dissolved organic carbon, permafrost degradation, carbon sources, Tibetan plateau

INTRODUCTION

Ground ice is substantially preserved in permafrost with an ice volume of 11.8–35.46×10^3 km^3 on the northern hemisphere (Zhang et al., 2000). Considerable amounts of dissolved carbon (DOC) locking in different ground ice are reported. For instance, high concentration of DOC (48–1,548 mg/L) is preserved in melting water of segregated ground ice in yedoma permafrost from central Alaska (Ewing et al., 2015a), and as much as 45.2 Tg DOC (with a maximum concentration of 28.6 mg/L) is stored in ice wedges in arctic yedoma permafrost regions (Fritz et al., 2015).

The current continuous global warming has resulted in the degradation of permafrost and subsequent melting of ground ice. The deepening of the active layer, melting of ground ice, and thermokarst processes lead to the decomposition and release of ancient DOC into aquatic systems (Vonk et al., 2015; Tanski et al., 2016). Notably, melting of ground ice accelerates the thawing of surrounding frozen sediments and concurrently brought OC, dissolved solutes, and microorganisms into ice meltwater, which would be an essential source of rivers and lakes (Connolly et al., 2020). Upon entering an aquatic system, DOC can be converted to CO_2 and emitted into the atmosphere, which would exert enormous influence on accelerating climate change and alternation of the biochemical cycle (Fritz et al., 2015; Selvam et al., 2017) in permafrost regions. The majority of studies on DOC mainly focused on ice wedges and massive ground ice (Vonk et al., 2013a; Fritz et al., 2015). Minor concern has been given to the pore ice.

The Tibetan Plateau (TP) is the largest region in a high-altitude setting. The permafrost stores as much as 12,700 km^3 of ground ice (Zhao et al., 2019). During recent decades, remarkable degradative trends of permafrost on the TP have been documented (Stocker et al., 2014; Ran et al., 2018). Decrease in ground ice content due to permafrost degradation facilitates the percolation of more water to deeper soil layers, thus resulting in the reallocation of runoff and water balance (Xu et al., 2008) and carbon distribution in the aquatic system and atmosphere (Guo et al., 2012; Chen et al., 2016; Mu et al., 2017; Ma et al., 2019). However, the current studies on the TP only focused on the soil carbon changes and stocks (Mu et al., 2015) in permafrost soils. Despite the vast amounts of ground ice volumes on the TP, little attention has been paid to the consequences of releasing DOC from melting ground ice, which has greatly underestimated the carbon budget in permafrost regions and could facilitate major ecosystem shifts on the TP. Under continuous warming and resultant permafrost degradation, considerable amounts of DOC in ground ice would release directly into the rivers and lakes to influence water quality of plateau and downstream recharge areas.

In this paper, we select the Source Area of Yellow River (SAYR) as our specific study area, which is often called the water tower of the Yellow River (Tian et al., 2015) and has experienced rapid degradation of permafrost. We aim to 1) expound the depth variations of DOC composition in high-resolution ground ice from two permafrost profiles in the SAYR; 2) trace the possible carbon sources and sequestration processes of DOC in the two profiles; and 3) discuss the consequences of DOC release from melting ice due to permafrost degradation in the SCG basin.

STUDY AREA AND SAMPLING SITES

The source area of the Yellow River (SAYR), defined as the catchment above the Tangnag Hydrological Station, is located on the northeastern TP (**Figure 1**). It provides as much as 34.5% of the total annual runoff with only 16.2% of areal extent (Lan et al., 2010), highlighting its importance for water resources
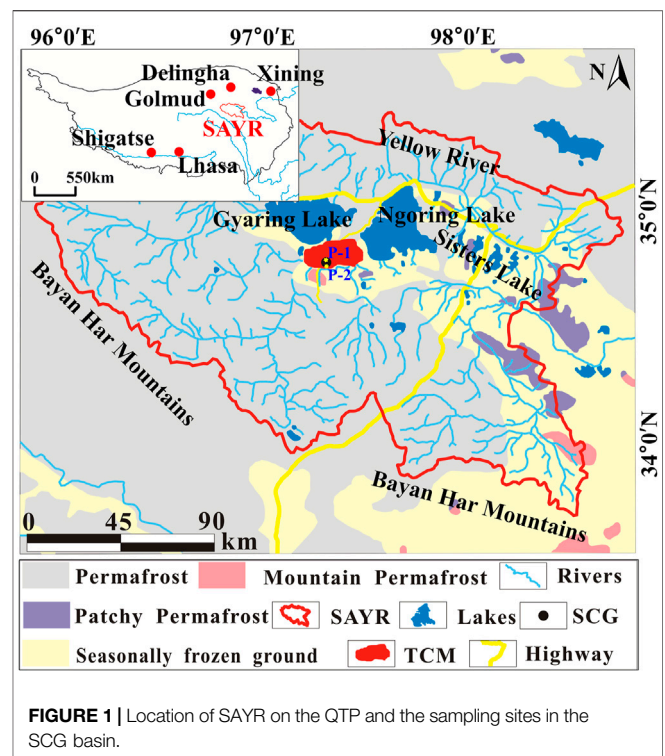

FIGURE 1 | Location of SAYR on the QTP and the sampling sites in the SCG basin.

managements and freshwater supply to the population in the middle and lower reaches of Yellow River. A mosaic of continuous, discontinuous, and sporadic permafrost as well as seasonally frozen ground is extensively distributed in the SAYR (Jin et al., 2009). Recent estimations reported a substantial reserve of ground ice between 3 and 10 m in the SAYR, reaching approximately 49.62 km^3 (Wang et al., 2017). According to field investigations and ground temperature records, permafrost in the SAYR is generally warm (>−1°) (Luo et al., 2014), and therefore vulnerable to thawing under continuous permafrost degradation, resulting in the release of dissolved solutes into surface water (Yang et al., 2019).

The Shuangchagou (SCG) basin was selected as our study site, near the southern bank of Ngoring Lake and Gyaring Lake (**Figure 1**). The landscape transition is remarkable in the SCG, which progresses from a desert steppe to an alpine meadow. Two streams are located in different ecosystems. The South branch is characterized by swampy alpine meadow, and the North branch flows through the desert steppe. Ice-rich permafrost is extensively developed, with ice content exceeding 60% (Yang et al., 2019). From 2014 to 2017, the annual average air temperature at SCG is −2.87°C, the total precipitation amount was 420 mm, and the average evaporation amount was as high as 1,000–1,500 mm. Two profiles (named as P-1 and P-2) with different vegetation and landform (Yang et al., 2019) at the SCG basin are dug to investigate the dissolved organic carbon (DOC) in ground ice. The P-1 (N 97°20′22.05″, E 34°39′14.1″, elevation: 4,455 m) is a palsa-like peat mound (**Figure 2A**), with more than 90% of alpine steppe dominating around this profile. Waters from around the peat mound and

FIGURE 2 | Landscapes for the two permafrost profiles **(A,B)** and sampling pictures **(C,D).**

the wetland water converge and flow into the Wanlongwoma River (**Figure 2A**), which remarkably influences the regional hydrological processes (Yang et al., 2019). Profile P-2 (N 97°19′44.36″, E 34°34′49.19″, elevation: 4,485 m) is on a flat terrain, exhibiting evident collapse in landscape of thermokarst gullies (**Figure 2B**). The predominant vegetation type is degraded alpine meadow (~90%). Continuous seepage was observed along this gully during our fieldwork, which was inferred to consist of summer rain, snowmelt water, and meltwater from thawing permafrost.

MATERIALS AND METHODS

Sampling Designations and Cryostratigraphic Record

To clarify the DOC distributions in ground ice, two sites presenting different landscapes (**Figure 2**) were designed at the SCG basin to investigate cryostratigraphy and obtain ground ice. Before excavation, the vegetation cover, topography, and hydrological conditions were investigated and photographically recorded (**Figure 2**). Two profiles were excavated manually using a shovel and an electric pick. The P-1 profile was excavated on top of a palsa-like frozen mound (**Figure 2A**; **Figure 2B**) with a height of ~2 m. Moreover, a thermal-erosion gully located 15 km apart from P-1 was chosen, and a profile (P-2) was dug from an exposed

slump crack (**Figure 2C**; **Figure 2D**). Two profiles were excavated to a depth of 4.8 m. The lithology, cryostructures, and ice conditions were documented and photographed before sampling. The frozen sediments and ice layers were cut using a chain saw and a chisel (**Figure 2B**; **Figure 2D**). The superficial layer of each sample was discarded to avoid any contamination. The profiles were cut in 5-cm intervals for P-1 (every 10 cm below 3 m) and 3-cm intervals for P-2.62, and 125 samples were collected in P-1 and P-2, respectively. In addition, the soil samples from the active layer and frozen layers were retrieved synchronously. All the samples were numbered in terms of depth, preserved in HDPE bottles, and kept frozen at –4°C in the field. In addition, five sites in the SCG basin were selected to collect the active layer water. Five pits were dug to a depth of 1.0 m, and the laterally and vertically permeated soil water were obtained in September (2014–2015) during our fieldwork.

Data Analysis Methods

The frozen samples were thawed entirely at 4°C, left until sediment settled, and then the liquid water above was filtered with pre-combusted GF/F filters and acidified (HCL, pH < 2) to prevent microbial conversion and to remove the carbonates. The DOC concentrations were measured with the solid and liquid modules of OI Analytical Analyzer (OI-Picarro, CA, United States), with a standard deviation of less than 0.5‰. The $\delta^{13}C_{DOC}$ values were analyzed with a Picarro Isotope

TABLE 1 | DOC and $\delta^{13}C_{DOC}$ in different water components on QTP.

Water components	Permafrost conditions[a]	Sample size	$\delta^{13}C_{DOC}$ (‰)			DOC (mg/L)			References
			Mean	Max	Min	Mean	Max	Min	
P–1	PF	62	−29.8	−27.4	−36.1	9.7	24.6	5.6	This study
P–2	PF	125	−31.6	−28.1	−36.9	21.5	70.1	8.8	This study
ALW	PF	169	−30.2	−26.1	−36.8	6.4	11.3	3.7	This study
LRW	PF	21	−25.6	−23.2	−26.9	2.3	7.1	0.2	1, 2, 3
	SFG	22	−25.8	−25.1	−26.9	1.2	2.6	0.2	2, 3, 4, 5
SSW	PF	26	−12.6	−10.7	−15.0	9.5	13.5	4.7	1, 6, 7, 8
SPW	— —	26	−21	−21	−21	0.6	1.3	0.2	9–12
PW	— —	11	−23	−21	−25	1.0	1.3	0.7	13–14
LLW	SFG	173	−25.6	−22.2	−28.8	2.8	8.1	0.5	4, 15
TLW	PF	9	−16.2	−15.1	−18.4	10.5	35.6	3.0	16
GW	PF	2	n.a.	n.a.	n.a.	11.9	15.0	8.8	2
	SFG	21	n.a.	n.a.	n.a.	1.3	3.8	0.3	2
GMW	— —	263	n.a.	n.a.	n.a.	1.2	2.2	0.2	9, 17, 18

[a]PF: permafrost; SFG: seasonal frozen ground.

1: Ma et al., 2018; 2: Hu et al., 2019; 3: Qu et al., 2017; 4: Kai et al., 2019; 5: Gao et al., 2019; 6: Liu et al., 2018; 7: Song et al., 2019; 8: Mu et al., 2017; 9: Yan et al., 2016; 10: Gao et al., 2020; 11: Liu et al., 2016; 12: Li Q. et al., 2018; 13: Li et al., 2017; 14: Li C. et al., 2018; 15: Su et al., 2018; 16: Mu et al., 2016; 17: Zhang et al., 2018; 18: Li X. et al., 2018.

Analyzer (Picarro G1102). Stable isotope results were expressed as δ values relative to the Vienna Peedee belemnite (VPDB) standard. The precision of $\delta^{13}C$ is <0.5‰, and the detection limit of DOC is 0.3 mg/L.

Total organic carbon (TOC) in sediments was measured using an OI Analytical model 1030 TOC analyzer (OI Analytical, United States). Each dry and homogenized sample was put into a small quartz boat after weighing. The 1 M HCl was added to the sample for 12 h to remove the carbonates. Then, the samples were heated to 900°C in the combustion chamber, and the organic matter in the samples was oxidized to CO_2 to measure the carbon contents.

Data Collection From Different Water Components

In order to clarify the potential origins of DOC in ground ice, the published data from different water components over the TP were collected and synthesized. Specifically, thermokarst lake water (TLW), glacial meltwater (GMW), small stream water (SSW), large river water (LRW), large lake water (LLW), precipitation water (PW), snowpit water (SPW), and groundwater (GW) at different sites were comprehensively investigated. The DOC and $\delta^{13}C$ (not available in GMW and GW) data were reanalyzed for comparison (**Table 1**; **Figure 5**).
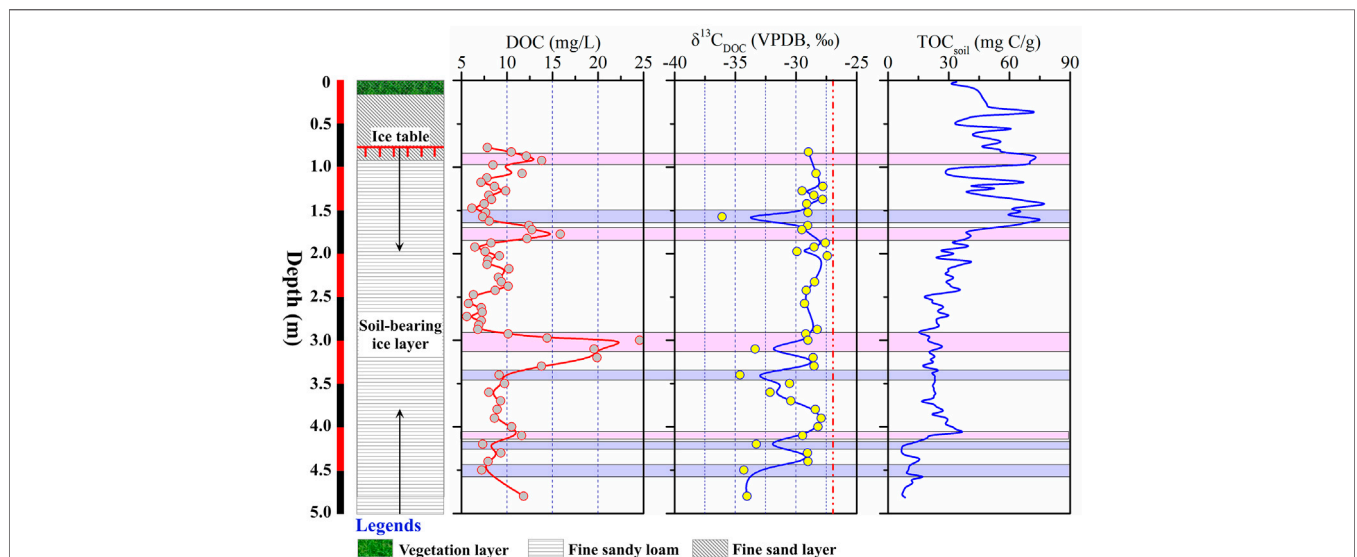

FIGURE 3 | Variations in DOC and $\delta^{13}C_{DOC}$ of ground ice and (total organic carbon) TOC of soil along depth in P-1. The pink bars represent four peaks of DOC in ground ice and the corresponding values of $\delta^{13}C$ and TOC_{soil}. The blue bars denote the lower DOC and more negative $\delta^{13}C$ values.
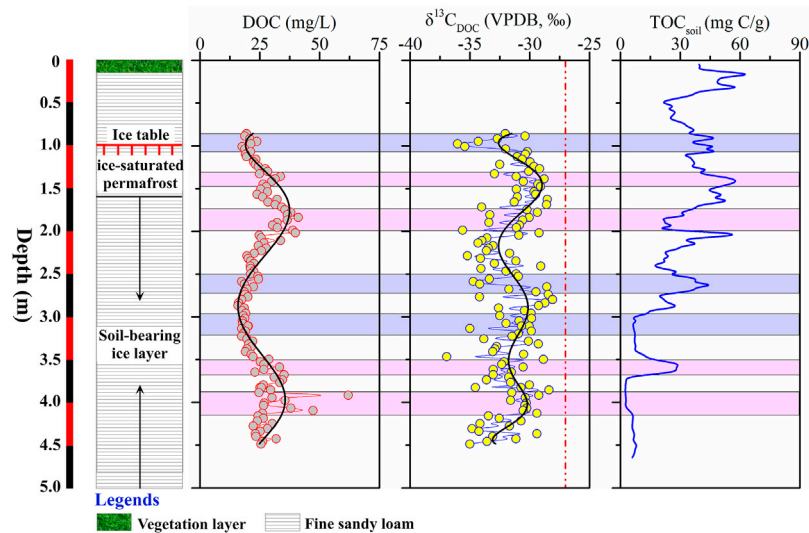
FIGURE 4 | Variations in DOC and $\delta^{13}C_{DOC}$ of ground ice and (total organic carbon) TOC of soil along depth in P-2. The pink bars represent four peaks of DOC in ground ice and the corresponding values of $\delta^{13}C$ and TOC_{soil}. The blue bars denote the lower DOC and more negative $\delta^{13}C$ values.
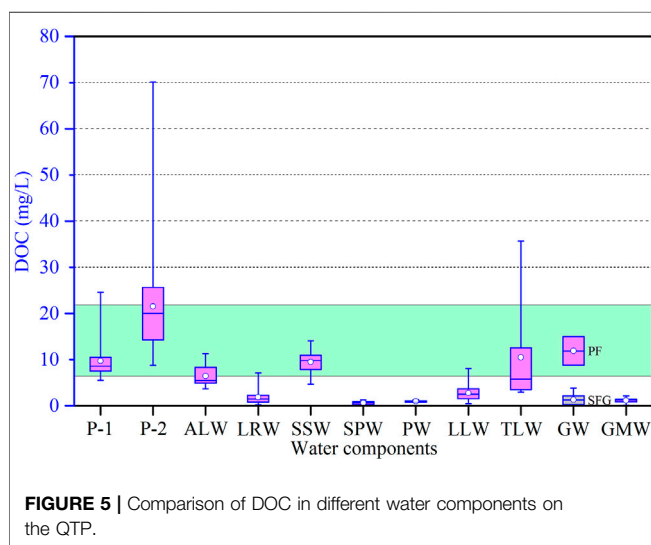

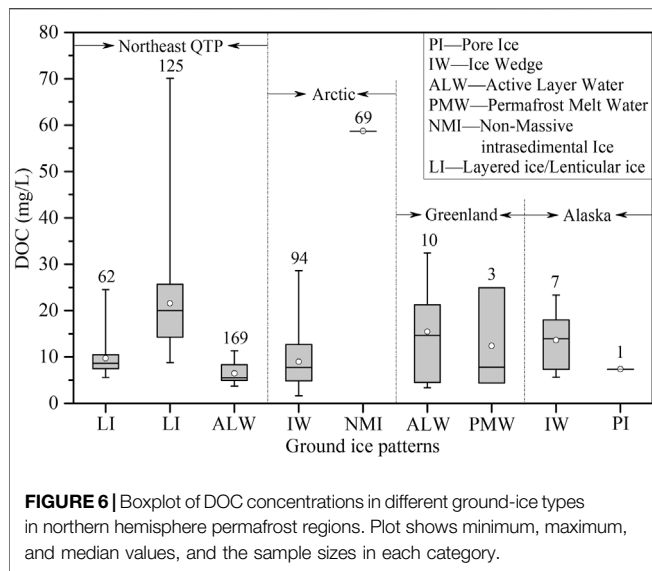**FIGURE 5 |** Comparison of DOC in different water components on the QTP.

RESULTS

Cryostratigraphy, Dissolved Organic Carbon and $\delta^{13}C_{DOC}$ of Ground Ice, and Total Organic Carbon of Soil in P-1

According to the field investigations, fine sandy soil is predominant in the upper layer and fine sandy loam dominates in the frozen layer in P-1 (**Figure 3**). Substantial soil-bearing ice layers are identified with volumetric ice contents ranging from 40% to 90% (**Figure 3**). The concentration of DOC ranges between 5.6 mg/L and 24.6 mg/L, with a mean of 9.7 mg/L. The peak DOC (24.6 mg/L) presents

at 3.0 m (**Figure 3**). The $\delta^{13}C_{DOC}$ varies from −27.4‰ to −36.1‰. Three higher DOC peaks are present at 0.9 m (13.8 mg/L), 1.8 m (15.8 mg/L), and 3.0 m (24.6 mg/L), corresponding to the relatively enriched $\delta^{13}C_{DOC}$ (pink bars in **Figure 3**). In contrast, the most negative $\delta^{13}C_{DOC}$ peaks appear at 1.6 m (−36.1‰), 3.1 m (−33.3‰), 3.4 m (−34.6‰), and 4.5 m (−34.3‰), which are consistent with the lower DOC contents (purple bars in **Figure 3**). However, higher DOC contents appear at 3.1 m, corresponding to the most negative $\delta^{13}C_{DOC}$ (green bar in **Figure 3**). In addition, the total organic carbon of soil (TOC_{soil}) in different depths was determined for comparison (**Figure 3**), the range of which is between 0.65% and 8.14%, with a mean value of 3.31%. The upper layer (0–1.6 m) contains much higher (mean level of 5.25%) and fluctuating TOC_{soil} than those in the deeper layers (**Figure 3**), suggesting the important influence of freeze–thaw cycle and evolution of permafrost/ground ice.

Cryostratigraphy, Dissolved Organic Carbon and $\delta^{13}C_{DOC}$ of Ground Ice, and Total Organic Carbon of Soil in P-2

For comparison, fine sandy loam layers dominated in the full profile for P-2 (**Figure 4**). Cryostratigraphy in this profile consists of ice-saturated permafrost (0.78–1.6 m) and soil-bearing ice layers (below 1.6 m), with volumetric ice contents ranging between 50% and 90%. The ground ice in P-2 presents higher DOC compared with P-1 (**Figure 4**). The DOC ranges between 8.8 and 70.1 mg/L, with a median of 21.5 mg/L. Moreover, the $\delta^{13}C_{DOC}$ ranges from −28.1‰ to −36.9‰, which is similar to that in P-1. There are three positive DOC peaks, located at 1.8 m, 2.2 m, and 4.1 m, respectively. Furthermore, $\delta^{13}C_{DOC}$ also shows some negative peaks (**Figure 4**). As for the ground ice in P-1, the DOC and $\delta^{13}C_{DOC}$ in P-2 show coincident trends, with higher DOC corresponding to the relatively enriched $\delta^{13}C_{DOC}$ and *vice*

FIGURE 6 | Boxplot of DOC concentrations in different ground-ice types in northern hemisphere permafrost regions. Plot shows minimum, maximum, and median values, and the sample sizes in each category.

Dissolved Organic Carbon Concentrations of Ground Ice in Different Types of Ground Ice

As shown in **Figure 6**, the highest contents of DOC (from 9.5 to 347.0 mg/L; mean: 58.7 mg/L) appear in the non-massive intrasedimental ice (NMI) in the arctic (Tanski et al., 2016; **Figure 6** and **Table 2**). However, the pore ice (PI) in Alaska (7.3 mg/L; Abbott et al., 2014) exhibited the lowest DOC concentration. Although the higher ice contents and huge volumes are found in ice wedges (IW) in the Arctic and Alaska, the DOC concentrations are not quite high as expected (**Figure 6**). By comparison, the layered ice and lenticular ice (LI) in the SAYR exhibit higher DOC concentrations, which are consistent with those in permafrost meltwater (PMW) and ALW. Specifically, the DOC concentrations in P-1 are consistent with the ice wedges, massive ice, and thermokarst exposed ice in the Arctic regions (Vonk et al., 2013a; Fritz et al., 2015; Tanski et al., 2016). However, the much higher concentrations of DOC in P-2 are close to those found in a localized thermal erosion ice wedge in Alaska (mean: 28.8 mg/L; Douglas et al., 2011).

DISCUSSION

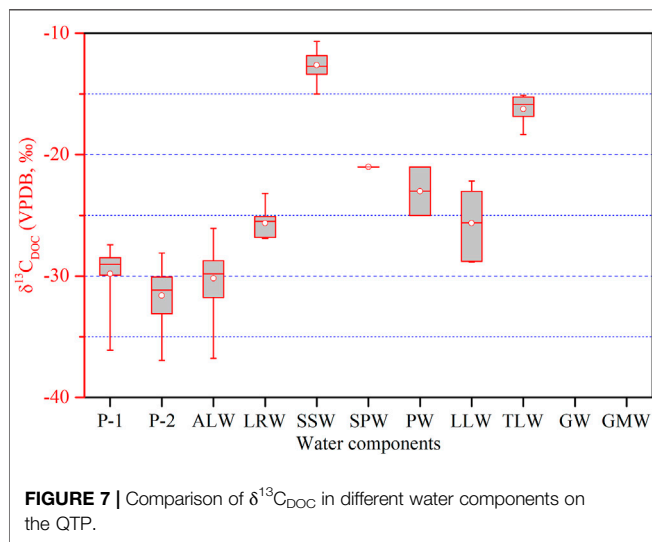## Possible Carbon Origins of Dissolved Organic Carbon in Ground Ice in the Shuangchagou

The carbon sources and accumulation processes of DOC in ground ice exert essential roles in the magnitude and bioavailability of DOC (Fritz et al., 2015). Generally, lower DOC concentrations in these types of ice were probably due to limited carbon inputs (Raymond and Bauer, 2000; Spencer et al., 2015), lower ice contents, and rapid *in situ* freezing (French and Shur, 2010). By contrast, the higher DOC concentrations of these ices are assumed to strongly interact with the higher ice contents and lacustrine origin of host sediments (Tanski et al., 2016). Importantly, the stable carbon isotopes ($\delta^{13}C_{DOC}$) for the initial source water of ground ice vary substantially. It was potentially due to various carbon input, local vegetation conditions, freeze fractionation (Cristea et al., 2014), ice formation patterns (Tanski et al., 2016), and different decomposition processes of organic carbon (Alewell et al., 2011). Accordingly, the $\delta^{13}C_{DOC}$ in ground ice can also be used to infer the carbon sources of ground ice.

As shown in **Figure 5**, the DOC concentrations in ground ice are similar to those of ALW, and the ^{13}C values are alike, indicating that the DOC in ground ice was closely related to the dissolving of organic matter from the active layer (Yu et al., 2017). The previous study also reported a similar DOC concentration of the soil solution in the upper active layer (26.3–39.5 mg/L) on the Northeastern Tibetan Plateau (NETP) (Luo et al., 2009) and substantial input (as high as 70%–94%)

versa. However, similarly opposite relations between DOC and $\delta^{13}C_{DOC}$ are identified at approximately 3.0 m, at which the lowest DOC concentrations correspond to the most enriched (median: −28.8‰) value of $\delta^{13}C_{DOC}$. Generally, the contents of TOC_{soil} in this profile exhibit remarkable variations with depth (**Figure 4**), ranging between 0.23% and 6.74%. Higher TOC_{soil} values (mean: 4.11%) appeared in the upper layer (0–1.7 m), which was similar to that in P-1, reflecting repeated freeze–thaw cycles and frequent exchange with external environment, resulting in carbon decomposition by microorganism. The frozen soil in the deep layer presents lower TOC_{soil} (mean: 1.95%).

Comparison of Dissolved Organic Carbon in Ground Ice and Other Water Components on the Tibetan Plateau

In order to determine the possible carbon sources of DOC in ground ice, the DOC data of different water components (including precipitation, snowpit, glacial meltwater, lakes, rivers, and groundwater) on the TP were collected for comparison (**Table 1**).

Remarkably, the ground ice in both profiles exhibits higher DOC concentrations (mean: 9.7–21.5 mg/L) than those in large river water (LRW) (mean: 1.2–2.3 mg/L), LLW (mean: 2.8 mg/L), snowpit water (SPW) (mean: 0.6 mg/L), precipitation water (PW) (mean: 1.0 mg/L), groundwater (GW) in seasonal frozen ground regions (mean: 1.3 mg/L), and glacial meltwater (GMW) (mean: 1.2 mg/L; **Table 1** and **Figure 5**). In comparison, the DOC of active layer water (ALW) (mean: 6.4 mg/L), small stream water (SSW) (mean: 9.5 mg/L), thermokarst lake water (TLW) (mean: 10.5 mg/L), and groundwater (GW) in permafrost regions (mean: 11.9 mg/L) is higher and comparable to that of ground ice (**Figure 5**), indicating connections between them and similar carbon behaviors with regard to the influence of permafrost.

TABLE 2 | Variations in the DOC concentration among different ground ice types.

Ice types	Monitor sites	Sample size	Mean DOC (mg/L)	References
LI	QTP	187	9.6–21.5	This study
IW	Arctic/Alaska	94/7	9.0/13.6	1, 2, 3
NMI	Arctic	69	58.7	2
PI	Alaska	1	7.3	3
PMW	Greenland	3	12.4	4
ALW	QTP/Greenland	169/10	6.4/15.4	This study/4

1: Fritz et al., 2015; 2: Tanski et al., 2016; 3: Abbott et al., 2014; 4: Leman, 2018.

FIGURE 7 | Comparison of $\delta^{13}C_{DOC}$ in different water components on the QTP.

FIGURE 8 | The DOC behaviors of ground ice along depth in both profiles. The gray bars represent the prominent DOC accumulation areas.

of OC from the active layer leachate to the permafrost streams (Wang et al., 2018). These kinds of DOC were usually originated from modern terrestrial biomass and surface organic layers (Guo et al., 2007). Due to the high hydraulic conductivity, low mineral content, and low DOC sorption capacity of the active layer soil (Striegl et al., 2005), the younger and biodegradable DOC (Drake et al., 2015) could migrate quickly to the permafrost table with limited microbial transformation. The DOC was easily sequestrated into the ground ice by freezing.

More depleted $\delta^{13}C_{DOC}$ values of ground ice in the SAYR (**Figure 7**; **Table 1**) are different from those of other water components on the TP. For comparison, the $\delta^{13}C_{DOC}$ values of ground ice (–31.6‰ to –29.8‰) are similar to ALW (–30.2‰), suggesting similar decomposition mechanisms and carbon sources. However, the $\delta^{13}C_{DOC}$ values of ground ice are much lower than the SSW and TLW (**Figure 7**), although melting ground ice was an important source of water for SSW and TLW (Yang et al., 2016; 2019). It suggests differences in carbon sources and decomposition processes under changing environments and distinct freezing conditions, which greatly influenced the stable isotopes of DOC (Krüger et al., 2014).

Notably, the mean values of measured $\delta^{13}C_{DOC}$ in the ground ice lie within the range of plants on the TP (Li
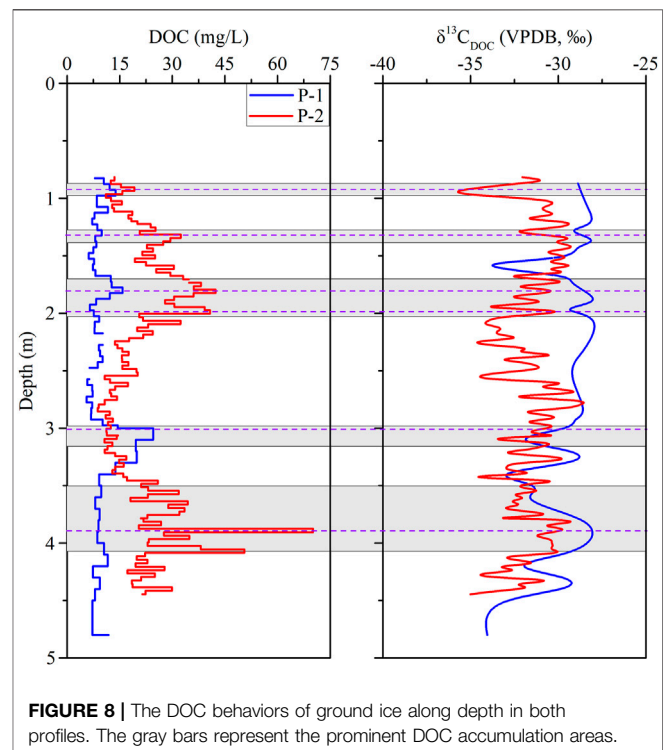
et al., 2007) and are similar (slightly depleted) to the values measured in $\delta^{13}C$ for moist soils on the northwestern TP (Mu et al., 2014). This suggests that all of the plants performed C_3 photosynthetic pathways with $\delta^{13}C$ values ranging from approximately –32‰ to –20‰ (Boutton, 1991; Farquhar et al., 1989; Raymond and Bauer., 2001). In addition, the consistent negative $\delta^{13}C_{DOC}$ values of ground ice and ALW (**Figure 7**) also suggest the leaching of organic matter from active layer soil. During water migration through the sediments of the active layer, the organic carbon of sediments and roots of plants melted out and subsequently dissolved into the supra-permafrost water, which sequestrated into ice during cold seasons (Guo and Macdonald, 2006; Guo et al., 2007; Tanski et al., 2016).

We thus conclude that the substantial leaching of DOC from organic layers and surrounding permafrost sediments are the important carbon sources of ground ice in the SAYR. Both freezing–thawing processes and permafrost evolution would

influence the embedding and sequestrating of DOC into ice. In addition, the microorganisms heterogeneously decomposed the organic carbon in permafrost and plants.

Sequestration Mechanisms of Dissolved Organic Carbon Into Ground Ice at Depths

The DOC and $\delta^{13}C_{DOC}$ composition show remarkable variations with depths (**Figure 3**; **Figure 4**), indicating different permafrost evolution processes and the resultant drivers of DOC incorporating into ice (Fritz et al., 2015), and the decomposition processes influenced by climate transition (Krüger et al., 2014). The depths with enriched $\delta^{13}C_{DOC}$ may reflect warm and wet climate conditions; in contrast, the lower $\delta^{13}C_{DOC}$ values reflect dry and cold conditions (Cristea et al., 2014). The higher DOC suggests quick freezing, and the lower DOC points towards the slow segregation, which excluded the solute in the water during ice formation.

As shown in **Figure 8**, the DOC in ground ice exhibits changing trends along depths, indicating different sequestration mechanisms of DOC during ice formation processes. As one of the most effective mechanisms for long-term carbon fixation in permafrost, freezing complicated the sequestrate process of DOC into ground ice. Meanwhile, the active layer properties, vegetation characteristics, and permafrost aggregation rates are also critical factors for DOC sequestration (Fritz et al., 2015).

Generally, the DOC of ground ice in the upper layers (1.6 m) presents gradually increasing DOC in both profiles, suggesting control of the freeze–thaw cycle. Below 1.6 m, the DOC and $\delta^{13}C_{DOC}$ exhibit fluctuating trends, suggesting alternating controls of permafrost evolution and the resultant ice formation mechanism under changing climate conditions (French and Pollar, 1986; Ewing et al., 2015a).

Specifically, the low DOC at P-1 and higher DOC at P-2 at 1.3 m (**Figure 8**) correspond to different ice formation mechanisms. The ice segregation process at P-1 and quick *in situ* freezing processes at P-2 are proposed. However, the second highest DOC peaks and enriched $\delta^{13}C_{DOC}$ at both P-1 and P-2 at approximately 1.8–2.0 m (**Figure 8**) are inferred to be affected by the warmer and wetter climate conditions (Cristea et al., 2014). The subsequent cold events at 1.9 ka (~2.2 m; Wang et al., 2018) promoted the upward aggradation of permafrost and quickly locked the DOC into ground ice. The much higher deposition rate at 2.0 m (Wang et al., 2018) also confirms the quick freezing processes.

At the depth of 3.1 m, the ground ice shows positive DOC peaks in both profiles, which follow depleted $\delta^{13}C_{DOC}$ values (**Figure 8**). As reported in Luo et al. (2018), the mean active layer thickness (ALT) in the SAYR is 2.8 m, and the repeated freeze–thaw cycles and microorganism activities in the active layer could significantly alter the DOC (Yu et al., 2017; Fuss et al., 2016). Also, the diverse carbon input and water availability from the external environment can influence the carbon isotopes in general (Cristea et al., 2014).

Between 3.5 and 4.3 m, the identical $\delta^{13}C_{DOC}$ trends in both profiles (**Figure 8**) suggest similar sequestration processes and

climate conditions (Porter et al., 2019). However, a high density of DOC at P-2 and a lower one at P-1 were observed, suggesting distinct ice formation mechanisms and organic carbon behaviors (i.e., decomposition, accumulation, and mixing). The P-1 is a palsa-like frozen mound; it was formed by an aggradation process (Krüger et al., 2014). The slow segregation processes at P-1 excluded the DOC from solid ice due to self-purification (Cheng, 1983). In contrast, P-2 exhibits an open-system feature, which could receive external water and produce a waterlogged and anaerobic environment. Thus, it reveals substantial accumulation of DOC in the ground ice, suggesting quick-freezing and efficiently locking of the DOC into the ice.

Significance of Dissolved Organic Carbon in Ground Ice on the Carbon Cycle Under Permafrost Degradation

As shown, the DOC concentrations of ground ice, TLW, SSW, and GW in permafrost regions are much higher than those of LLW and LRW in seasonal frozen ground regions (**Figure 9**), which may be significantly related to the degradation of permafrost with high-content ground ice. For comparison, the ice contents in the seasonally frozen ground are usually lower (Zhou et al., 2000; Zou et al., 2017) and are commonly surrounded by thick unfrozen sediments, so the influence of thawing permafrost is thus negligible. Previous studies on the TP suggested that the contribution of melting ground ice to thermokarst lakes were as high as 37.75%–51.75% (Yang et al., 2016), and the melting ground ice similarly provided 13.2%–16.7% of total discharges to the streams (Yang et al., 2019). It has been suggested that permafrost thaw has released substantial melt water, bringing massive labile DOC into streams (Gao et al., 2019; Song et al., 2019) and thermokarst lakes (Mu et al., 2016) on the TP.

During recent decades, the SAYR has been undergoing remarkable permafrost degradation due to continuous temperature rise (Jin et al., 2009). A gradual increase in ALT at a rate of 2.2 cm/a in the SAYR was determined (Luo et al., 2014). Note that these rates of permafrost degradation in the SAYR are sizably higher than those in the interior TP (Jin et al., 2009), which resulted in massive melting of ground ice. On the one hand, the excess ground ice would release a large amount of meltwater to recharge the surface runoff and lakes (Lee et al., 2014) and simultaneously release a considerable DOC flux into the freshwater system (Vonk et al., 2015), which can be used by plant roots (Becker et al., 2016; **Figure 9**). On the other hand, the melting of ground ice increased the soil pore (Walvoord and Kurylyk, 2016) and allowed much more supra-permafrost water, precipitation, and surface water to infiltrate into the deep permafrost (Yang et al., 2017). These waters could penetrate deeply through taliks to connect with the sub-permafrost water, and further leached labile carbon from the ambient frozen sediments (**Figure 9**). During this process, the DOC in shallow layers could enter the sub-permafrost water *via* taliks. These activities substantially altered the DOC dynamics in permafrost (ground ice) and aquatic systems (**Figure 9**).
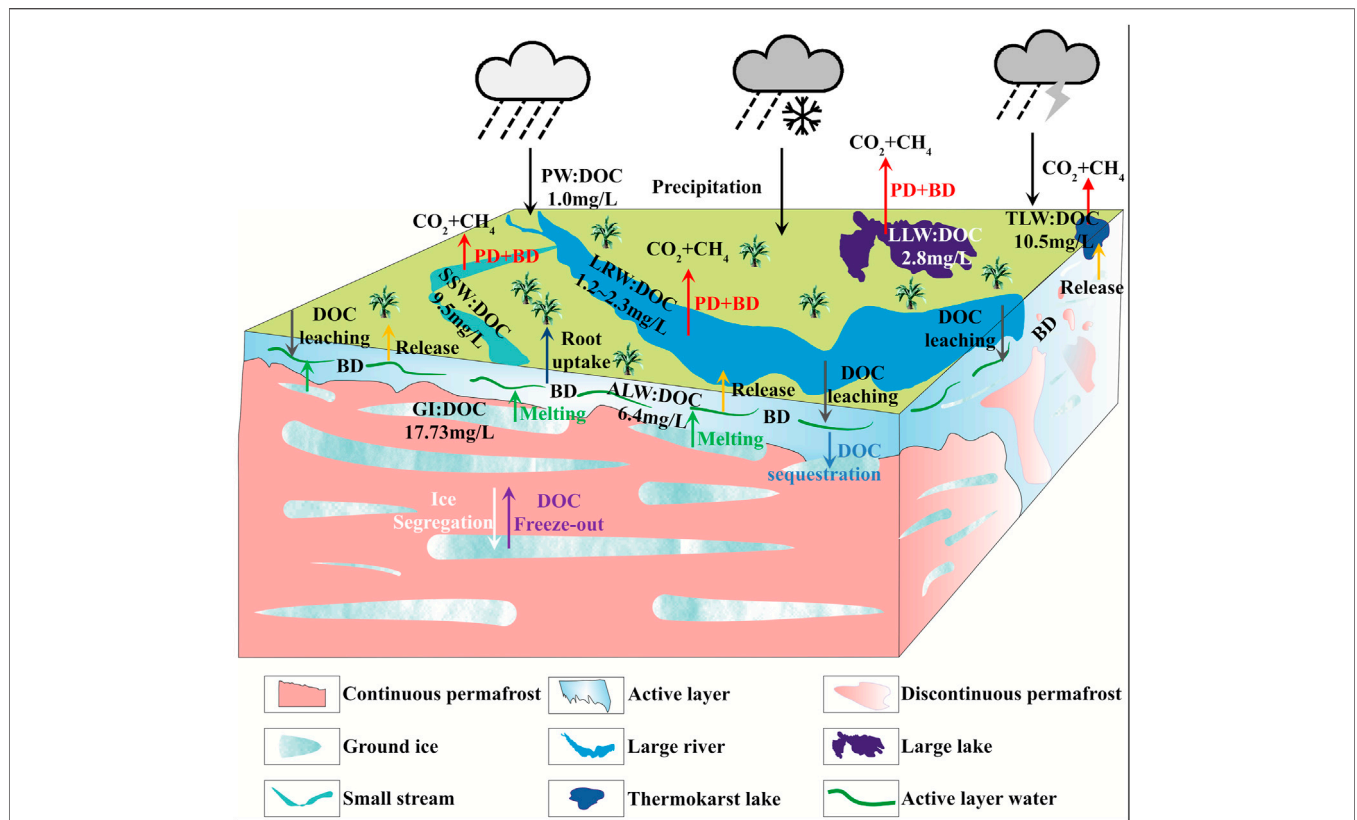
FIGURE 9 | Conceptual diagram of DOC dynamics under permafrost thaw in the SAYR. BD and PD stand for biochemical degradation and photo degradation.

Importantly, continuous permafrost would degrade into discontinuous permafrost and finally change into seasonally frozen ground. The GW in permafrost regions presents higher DOC levels than that in seasonally frozen ground regions (**Figure 5**), which is closely related to the occurrence of ground ice. Accordingly, the transition from permafrost to seasonal frozen ground will greatly influence the thermal regimes of large lakes and large rivers distributing in seasonal frozen ground regions, ultimately leading to a great increase in DOC of LLW and LRW (**Figure 9**). Because the DOC from ground ice is chemically labile (Vonk et al., 2013a), it can be decomposed easily by microbial and photochemical processes after entering into lakes and rivers (Battin et al., 2008; Vonk et al., 2013a) and finally released to the atmosphere (**Figure 9**).

CONCLUSION AND OUTLOOK

In this study, the high-resolution DOC data in ground ice from two permafrost profiles in the SAYR were firstly shown, the origins and sequestrations of DOC in ground ice were investigated, and the potential influence of DOC on the carbon cycle upon permafrost thaw were discussed. The following conclusions can be drawn:

1) Remarkable depth differences in the ground ice DOC and $\delta^{13}C_{DOC}$ were found for both sites. The ground ice in upper layers (0–1.6 m) exhibits higher DOC concentrations rather than those in deeper layers (>1.6 m), which is related to the active layer hydrology and freeze–thaw cycles. However, the origins and sequestration processes of DOC in the deeper ground ice were complex, which is closely related to the evolution of ice, the carbon behaviors of the ambient water (Fritz et al., 2015).

2) Our conceptual model emphasizes the significant contribution of DOC in ground ice to the carbon cycle in the SAYR. Considering the important water conservation area in China and the sensitive regions to climate warming, the release of DOC from ground ice in the SAYR will be significant under continuous permafrost degradation.

3) Due to the limitation of ground ice reserve data and lack of mass investigations of DOC in ground ice on a large scale in the SAYR, accurate evaluation of DOC budgets in ground ice in the SAYR is hard to estimate. Accordingly, future work is indispensable to investigate the general distribution and storage of DOC in ground ice on regional scales on the TP.

This work is the first and preliminary attempt at carrying out a DOC study on ground ice on the TP. These results serve as a call for other studies to include the carbon cycle on the TP as an underpinning to comprehend the behavior of permafrost-related

organic carbon, and incorporate this variation into projections of future climate change.

DATA AVAILABILITY STATEMENT

The original contributions presented in the study are included in the article/Supplementary Material. Further inquiries can be directed to the corresponding authors.

AUTHOR CONTRIBUTIONS

YY and XG: Conceptualization, Methodology, Investigation, and Writing—review and editing. QW: Data analysis. HJ: review and editing. HY: Data analysis. QW: Supervision and editing.

FUNDING

ACKNOWLEDGMENTS

REFERENCES

Abbott, B. W., Larouche, J. R., Jones, J. B., Bowden, W. B., and Balser, A. W. (2014). Elevated Dissolved Organic Carbon Biodegradability from Thawing and Collapsing Permafrost. *J. Geophys. Res. Biogeosci.* 119 (10), 2049–2063. doi:10.1002/2014jg002678

Alewell, C., Giesler, R., Klaminder, J., Leifeld, J., and Rollog, M. (2011). Stable Carbon Isotopes as Indicators for Environmental Change in Palsa Peats. *Biogeosciences* 8 (7), 1769–1778. doi:10.5194/bg-8-1769-2011

Battin, T. J., Kaplan, L. A., Findlay, S., Hopkinson, C. S., Marti, E., Packman, A. I., et al. (2008). Biophysical Controls on Organic Carbon Fluxes in Fluvial Networks. *Nat. Geosci* 1, 95–100. doi:10.1038/ngeo101

Becker, M. S., Davies, T. J., and Pollard, W. H. (2016). Ground Ice Melt in the High Arctic Leads to Greater Ecological Heterogeneity. *J. Ecol.* 104 (1), 114–124. doi:10.1111/1365-2745.12491

Boutton, T. W. (1991). Stable Carbon Isotope Ratios of Natural Materials: II. Atmospheric, Terrestrial, Marine, and Freshwater Environments. *Carbon Isotope Techniques.* Academic Press Inc., 173–185.

Chen, L., Liang, J., Qin, S., Liu, L., Fang, K., Xu, Y., et al. (2016). Determinants of Carbon Release from the Active Layer and Permafrost Deposits on the Tibetan Plateau. *Nat. Commun.* 7, 1–12. doi:10.1038/ncomms13046

Connolly, C. T., Cardenas, M. B., Burkart, G. A., Spencer, R. G. M., and McClelland, J. W. (2020). Groundwater as a Major Source of Dissolved Organic Matter to Arctic Coastal Waters. *Nat. Commun.* 11 (1), 1–8. doi:10.1038/s41467-020-15250-8

Cristea, G., Cuna, S. M., Fărcaş, S., Tanţău, I., Dordai, E., and Măgdaş, D. A. (2014). Carbon Isotope Composition as Indicator for Climatic Changes during the Middle and Late Holocene in a Peat Bog from Maramureş Mountains (Romania). *The Holocene* 24 (1), 15–23. doi:10.1177/0959683613512166

Douglas, T. A., Fortier, D., Shur, Y. L., Kanevskiy, M. Z., Guo, L., Cai, Y., et al. (2011). Biogeochemical and Geocryological Characteristics of Wedge and Thermokarst-Cave Ice in the CRREL Permafrost Tunnel, Alaska. *Permafrost Periglac. Process.* 22 (2), 120–128. doi:10.1002/ppp.709

Drake, T. W., Wickland, K. P., Spencer, R. G. M., McKnight, D. M., and Striegl, R. G. (2015). Ancient Low-Molecular-Weight Organic Acids in Permafrost Fuel Rapid Carbon Dioxide Production upon Thaw. *Proc. Natl. Acad. Sci. USA* 112, 13946–13951. doi:10.1073/pnas.1511705112

Ewing, S. A., O'Donnell, J. A., Aiken, G. R., Butler, K., Butman, D., Windham-Myers, L., et al. (2015a). Long-term Anoxia and Release of Ancient, Labile Carbon upon Thaw of Pleistocene Permafrost. *Geophys. Res. Lett.* 42 (24), 10730–10738. doi:10.1002/2015gl066296

Farquhar, G. D., Ehleringer, J. R., and Hubick, K. T. (1989). Carbon Isotope Discrimination and Photosynthesis. *Annu. Rev. Plant Physiol. Plant Mol. Biol.* 40 (1), 503–537. doi:10.1146/annurev.pp.40.060189.002443

French, H. M., and Pollard, W. H. (1986). Ground-ice Investigations, Klondike District, Yukon Territory. *Can. J. Earth Sci.* 23 (4), 550–560. doi:10.1139/e86-055

French, H., and Shur, Y. (2010). The Principles of Cryostratigraphy. *Earth-Science Rev.* 101 (3-4), 190–206. doi:10.1016/j.earscirev.2010.04.002

Fritz, M., Opel, T., Tanski, G., Herzschuh, U., Meyer, H., Eulenburg, A., et al. (2015). Dissolved Organic Carbon (DOC) in Arctic Ground Ice. *The Cryosphere* 9, 737–752. doi:10.5194/tc-9-737-2015

Gao, T., Kang, S., Zhang, Y., Sprenger, M., Wang, F., Du, W., et al. (2020). Characterization, Sources and Transport of Dissolved Organic Carbon and Nitrogen from a Glacier in the Central Asia. *Sci. Total Environ.* 725, 138346. doi:10.1016/j.scitotenv.2020.138346

Gao, T., Kang, S., Chen, R., Zhang, T., Zhang, T., Han, C., et al. (2019). Riverine Dissolved Organic Carbon and its Optical Properties in a Permafrost Region of the Upper Heihe River basin in the Northern Tibetan Plateau. *Sci. total Environ.* 686, 370–381. doi:10.1016/j.scitotenv.2019.05.478

Guo, D., Wang, H., and Li, D., 2012. A Projection of Permafrost Degradation on the Tibetan Plateau during the 21st century: Projection of Permafrost Degradation. *J. Geophys. Res.* 117. 16545. doi:10.1029/2011JD016545

Guo, L., and Macdonald, R. W. (2006). Source and Transport of Terrigenous Organic Matter in the Upper Yukon River: Evidence from Isotope ($\delta^{13}C$, $\Delta^{14}C$, and $\delta^{15}N$) Composition of Dissolved, Colloidal, and Particulate Phases. *Global Biogeochem. Cycles* 20, 1–12. doi:10.1029/2005gb002593

Guo, L., Ping, C. L., and Macdonald, R. W. (2007). Mobilization Pathways of Organic Carbon from Permafrost to Arctic Rivers in a Changing Climate. *Geophys. Res. Lett.* 34 (13), L13603. doi:10.1029/2007gl030689

Guodong, C. (1983). The Mechanism of Repeated-Segregation for the Formation of Thick Layered Ground Ice. *Cold Regions Sci. Tech.* 8 (1), 57–66. doi:10.1016/0165-232x(83)90017-4

Hu, Y. L. (2019). *PhD Thesis.Impacts of the Groundwater Flow Path on the Patterns of Dissolved Organic Carbon Export in the Cold Alpine Area.* Wuhan: China University of Geosciences, 1–134

Jin, H., He, R., Cheng, G., Wu, Q., Wang, S., Lü, L., et al. (2009). Changes in Frozen Ground in the Source Area of the Yellow River on the Qinghai–Tibet Plateau, China, and Their Eco-Environmental Impacts. *Environ. Res. Lett.* 4, 045206.

Kai, J. L., Wang, J. B., Huang, L., Wang, Y., Ju, J. T., and Zhu, L. P. (2019). Seasonal Variations of Dissolved Organic Carbon and Total Nitrogen Concentrations in Nam Co and Inflowing Rivers, Tibet Plateau. *J. Lake Sci.* 31 (4), 1099–1108.

Krüger, J. P., Leifeld, J., and Alewell, C. (2014). Degradation Changes Stable Carbon Isotope Depth Profiles in Palsa Peatlands. *Biogeosciences* 11, 3369–3380. doi:10.5194/bg-11-3369-2014

Lan, Y., Zhao, G., Zhang, Y., Wen, J., Liu, J., and Hu, X. (2010). Response of Runoff in the Source Region of the Yellow River to Climate Warming. *Quat. Int.* 226 (1-2), 60–65. doi:10.1016/j.quaint.2010.03.006

Lee, H., Swenson, S. C., Slater, A. G., and Lawrence, D. M. (2014). Effects of Excess Ground Ice on Projections of Permafrost in a Warming Climate. *Environ. Res. Lett.* 9, 124006. doi:10.1088/1748-9326/9/12/124006

Li, C., Chen, P., Kang, S., Yan, F., Tripathee, L., Wu, G., et al. (2018b). Fossil Fuel Combustion Emission from South Asia Influences Precipitation Dissolved Organic Carbon Reaching the Remote Tibetan Plateau: Isotopic and Molecular Evidence. *J. Geophys. Res. Atmos.* 123 (11), 6248–6258. doi:10.1029/2017jd028181

Li, C., Yan, F., Kang, S., Chen, P., Hu, Z., Han, X., et al. (2017). Deposition and Light Absorption Characteristics of Precipitation Dissolved Organic Carbon (DOC) at Three Remote Stations in the Himalayas and Tibetan Plateau, China. *Sci. Total Environ.* 605-606, 1039–1046. doi:10.1016/j.scitotenv.2017.06.232

Li, M., Liu, H., Li, L., Yi, X., and Zhu, X. (2007). Carbon Isotope Composition of Plants along Altitudinal Gradient and its Relationship to Environmental Factors on the Qinghai-Tibet Plateau. *Polish J. Ecol.* 55 (1), 67–78.

Li, Q., Wang, N., Barbante, C., Kang, S., Yao, P., Wan, X., et al. (2018a). Levels and Spatial Distributions of Levoglucosan and Dissolved Organic Carbon in Snowpits over the Tibetan Plateau Glaciers. *Sci. Total Environ.* 612, 1340–1347. doi:10.1016/j.scitotenv.2017.08.267

Li, X., Ding, Y., Xu, J., He, X., Han, T., Kang, S., et al. (2018c). Importance of Mountain Glaciers as a Source of Dissolved Organic Carbon. *J. Geophys. Res. Earth Surf.* 123 (9), 2123–2134. doi:10.1029/2017jf004333

Liu, F., Chen, L., Zhang, B., Wang, G., Qin, S., and Yang, Y. (2018). Ultraviolet Radiation rather Than Inorganic Nitrogen Increases Dissolved Organic Carbon Biodegradability in a Typical Thermo-Erosion Gully on the Tibetan Plateau. *Sci. Total Environ.* 627, 1276–1284. doi:10.1016/j.scitotenv.2018.01.275

Luo, C., Xu, G., Wang, Y., Wang, S., Lin, X., and Hu, Y. (2009). Effects of Grazing and Experimental Warming on DOC Concentrations in the Soil Solution on the Qinghai-Tibet Plateau. *Soil Biol. Biochem.* 41 (12), 2493–2500. doi:10.1016/j.soilbio.2009.09.006

Luo, D., HuiJun, J., Marchenko, S., and Romanovsky, V. (2014). Distribution and Changes of Active Layer Thickness (ALT) and Soil Temperature (TTOP) in the Source Area of the Yellow River Using the GIPL Model. *Sci. China Earth Sci.* 57 (8), 1834–1845. doi:10.1007/s11430-014-4852-1

Ma, Q., Jin, H., Yu, C., and Bense, V. F. (2019). Dissolved Organic Carbon in Permafrost Regions: A Review. *Science China Earth Sciences* 62 (2), 349–364. doi:10.1007/s11430-018-9309-6

Mu, C. C., Abbott, B. W., Wu, X. D., Zhao, Q., Wang, H. J., Su, H., et al. (2017). Thaw Depth Determines Dissolved Organic Carbon Concentration and Biodegradability on the Northern Qinghai-Tibetan Plateau. *Geophys. Res. Lett.* 44 (18), 9389–9399. doi:10.1002/2017gl075067

Mu, C., Zhang, T., Wu, Q., Peng, X., Cao, B., Zhang, X., et al. (2015). Organic Carbon Pools in Permafrost Regions on the Qinghai–Xizang (Tibetan) Plateau. *The Cryosphere* 9 (2), 479–486. doi:10.5194/tc-9-479-2015

Mu, C., Zhang, T., Wu, Q., Zhang, X., Cao, B., Wang, Q., et al. (2014). Stable Carbon Isotopes as Indicators for Permafrost Carbon Vulnerability in Upper Reach of Heihe River basin, Northwestern China. *Quat. Int.* 321, 71–77. doi:10.1016/j.quaint.2013.12.001

Mu, C., Zhang, T., Zhang, X., Li, L., Guo, H., Zhao, Q., et al. (2016). Carbon Loss and Chemical Changes from Permafrost Collapse in the Northern Tibetan Plateau: Permafrost Collapse Caused Carbon Loss. *J. Geophys. Res. Biogeosci* 121, 1781–1791. doi:10.1002/2015jg003235

Qu, B., Sillanpää, M., Li, C., Kang, S., Stubbins, A., Yan, F., et al. 2017. Aged Dissolved Organic Carbon Exported from Rivers of the Tibetan Plateau. *PloS one*, 12.1–11.doi:10.1371/journal.pone.0178166

Ran, Y., Li, X., and Cheng, G. (2018). Climate Warming over the Past Half century Has Led to thermal Degradation of Permafrost on the Qinghai–Tibet Plateau. *The Cryosphere* 12 (2), 595. doi:10.5194/tc-12-595-2018

Raymond, P. A., and Bauer, J. E. (2000). Bacterial Consumption of DOC during Transport through a Temperate Estuary. *Aquat. Microb. Ecol.* 22 (1), 1–12. doi:10.3354/ame022001

Raymond, P. A., and Bauer, J. E. (2001). Riverine export of Aged Terrestrial Organic Matter to the North Atlantic Ocean. *Nature* 409 (6819), 497–500. doi:10.1038/35054034

Selvam, B. P., Lapierre, J. F., Guillemette, F., Voigt, C., Lamprecht, R. E., Biasi, C., et al. (2017). Degradation Potentials of Dissolved Organic Carbon (DOC) from Thawed Permafrost Peat. *Scientific Rep.* 7, 45811. doi:10.1038/srep45811

Song, C., Wang, G., Mao, T., Chen, X., Huang, K., Sun, X., et al. (2019). Importance of Active Layer Freeze-Thaw Cycles on the Riverine Dissolved Carbon export on the Qinghai-Tibet Plateau Permafrost Region. *PeerJ* 7, e7146. doi:10.7717/peerj.7146

Spencer, R. G., Mann, P. J., Dittmar, T., Eglinton, T. I., McIntyre, C., and Holmes, R. M. (2015). Detecting the Signature of Permafrost Thaw in Arctic Rivers. *Geophys. Res. Lett.* 42 (8), 2830–2835. doi:10.1002/2015gl063498

Stocker, T. (2014) Edition. Climate Change 2013: the Physical Science Basis: Working Group I Contribution to the Fifth Assessment Report of the Intergovernmental Panel on Climate Change. Cambridge university press.

Striegl, R. G., Aiken, G. R., Dornblaser, M. M., Raymond, P. A., and Wickland, K. P. (2005). A Decrease in Discharge-Normalized DOC export by the Yukon River during Summer through Autumn. *Geophys. Res. Lett.* 32, 413. doi:10.1029/2005gl024413

Su, Y., Hu, E., Liu, Z., Jeppesen, E., and Middelburg, J. J. (2018). Assimilation of Ancient Organic Carbon by Zooplankton in Tibetan Plateau Lakes Is Depending on Watershed Characteristics. *Limnology and Oceanography* 63 (6), 2359–2371. doi:10.1002/lno.10943

Tanski, G., Couture, N., Lantuit, H., Eulenburg, A., and Fritz, M. (2016). Eroding Permafrost Coasts Release Low Amounts of Dissolved Organic Carbon (DOC) from Ground Ice into the Nearshore Zone of the Arctic Ocean. *Glob. Biogeochem. Cycles* 30 (7), 1054–1068. doi:10.1002/2015gb005337

Tian, H., Lan, Y., Wen, J., Jin, H., Wang, C., Wang, X., et al. (2015). Evidence for a Recent Warming and Wetting in the Source Area of the Yellow River (SAYR) and its Hydrological Impacts. *J. Geographical Sci.* 25 (6), 643–668. doi:10.1007/s11442-015-1194-7

Vonk, J. E., Mann, P. J., Dowdy, K. L., Davydova, A., Davydov, S. P., Zimov, N., et al. (2013a). Dissolved Organic Carbon Loss from Yedoma Permafrost Amplified by Ice Wedge Thaw. *Environ. Res. Lett.* 8, 035023. doi:10.1088/1748-9326/8/3/035023

Vonk, J. E., Tank, S. E., Bowden, W. B., Laurion, I., Vincent, W. F., Alekseychik, P., et al. (2015). Reviews and Syntheses: Effects of Permafrost Thaw on Arctic Aquatic Ecosystems. *Biogeosciences* 12 (23), 7129–7167. doi:10.5194/bg-12-7129-2015

Walvoord, M. A., and Kurylyk, B. L. (2016). Hydrologic Impacts of Thawing Permafrost—A Review. *Vadose Zone J.* 15 (6), 1–20. doi:10.2136/vzj2016.01.0010

Wang, S. T., Sheng, Y., Cao, W., Li, J., Ma, S., and Hu, X. Y. (2017). Estimation of Permafrost Ice Reserves in the Source Area of the Yellow River Using Landform Classification. *Adv. Water Sci.* 28 (6), 801–810.

Wang, Y., Spencer, R. G., Podgorski, D. C., Kellerman, A. M., Rashid, H., and Zito, P. (2018). Spatiotemporal Transformation of Dissolved Organic Matter along an alpine Stream Flow Path on the Qinghai–Tibet Plateau: Importance of Source and Permafrost Degradation. *Biogeosciences* 15 (21), 6637–6648. doi:10.5194/bg-15-6637-2018

Xu, X., Lu, C., Shi, X., and Gao, S. (2008). World Water tower: an Atmospheric Perspective. *Geophys. Res. Lett.* 35, L20815.

Yan, F., Kang, S., Li, C., Zhang, Y., Qin, X., Li, Y., et al. (2016). Concentration, Sources and Light Absorption Characteristics of Dissolved Organic Carbon on a Medium-Sized valley Glacier. *Northern Tibetan Plateau. Cryosphere* 10.

Yang, Y., Wu, Q., Hou, Y., Zhang, Z., Zhan, J., Gao, S., et al. (2017). Unraveling of Permafrost Hydrological Variabilities on Central Qinghai-Tibet Plateau Using Stable Isotopic Technique. *Sci. Total Environ.* 605, 199–210. doi:10.1016/j.scitotenv.2017.06.213

Yang, Y., Wu, Q., Jin, H., Wang, Q., Huang, Y., Luo, D., et al. (2019). Delineating the Hydrological Processes and Hydraulic Connectivities under Permafrost Degradation on Northeastern Qinghai-Tibet Plateau, China. *J. Hydrol.* 569, 359–372. doi:10.1016/j.jhydrol.2018.11.068

Yang, Y., Wu, Q., Yun, H., Jin, H., and Zhang, Z. (2016). Evaluation of the Hydrological Contributions of Permafrost to the Thermokarst Lakes on the Qinghai–Tibet Plateau Using Stable Isotopes. *Glob. Planet. Change* 140, 1–8. doi:10.1016/j.gloplacha.2016.03.006

Yu, S.-Y., He, H., Cheng, P., and Hou, Z. (2017). Depth Heterogeneity of Soil Organic Carbon Dynamics in a Heavily Grazed alpine Meadow on the Northeastern Tibetan Plateau: A Radiocarbon-Based Approach,. *J. Geophys. Res. Biogeosci.* 122, 1775–1788. doi:10.1002/2016JG003567

Zhang, T., Heginbottom, J. A., Barry, R. G., and Brown, J. (2000). Further Statistics on the Distribution of Permafrost and Ground Ice in the Northern Hemisphere. *Polar Geogr.* 24 (2), 126–131. doi:10.1080/10889370009377692

Zhang, Y., Kang, S., Li, G., Gao, T., Chen, P., Li, X., et al. (2018). Dissolved Organic Carbon in Glaciers of the southeastern Tibetan Plateau: Insights into Concentrations and Possible Sources. *PloS one* 13, e0205414.

Zhao, L., Hu, G., Zou, D., Wu, X., Ma, L., Sun, Z., et al. (2019). Permafrost Changes and its Effects on Hydrological Processes on Qinghai-Tibet Plateau. *Bull. Chin. Acad. Sci.* 34 (11), 1233–1246.

Zhou, Y. W., Guo, D. X., Qiu, G. Q., Cheng, G. D., and Li, S. D. (2000). *Geocryology in China*. Beijing: Science Press.

Zou, D., Zhao, L., Yu, S., Chen, J., Hu, G., Wu, T., et al. (2017). A New Map of Permafrost Distribution on the Tibetan Plateau. *The Cryosphere* 11 (6), 2527–2542. doi:10.5194/tc-11-2527-2017

Conflict of Interest: The authors declare that the research was conducted in the absence of any commercial or financial relationships that could be construed as a potential conflict of interest.

Publisher's Note: All claims expressed in this article are solely those of the authors and do not necessarily represent those of their affiliated organizations, or those of the publisher, the editors, and the reviewers. Any product that may be evaluated in this article, or claim that may be made by its manufacturer, is not guaranteed or endorsed by the publisher.